Adipogenesis is inhibited by brief, daily exposure to high-frequency, extremely low-magnitude mechanical signals

C. T. Rubin*†, E. Capilla‡, Y. K. Luu*, B. Busa*, H. Crawford‡, D. J. Nolan§¶, V. Mittal§¶, C. J. Rosen‖, J. E. Pessin‡, and S. Judex*

Departments of *Biomedical Engineering and ‡Pharmacology and ¶Graduate Program in Genetics, Stony Brook University, Stony Brook, NY 11794; §Cold Spring Harbor Laboratory, Cold Spring Harbor, NY 11724; and ‖The Jackson Laboratory, Bar Harbor, ME 04609

Communicated by William J. Lennarz, Stony Brook University, Stony Brook, NY, September 19, 2007 (received for review June 20, 2007)

Obesity, a global pandemic that debilitates millions of people and burdens society with tens of billions of dollars in health care costs, is deterred by exercise. Although it is presumed that the more strenuous a physical challenge the more effective it will be in the suppression of adiposity, here it is shown that 15 weeks of brief, daily exposure to high-frequency mechanical signals, induced at a magnitude well below that which would arise during walking, inhibited adipogenesis by 27% in C57BL/6J mice. The mechanical signal also reduced key risk factors in the onset of type II diabetes, nonesterified free fatty acid and triglyceride content in the liver, by 43% and 39%, respectively. Over 9 weeks, these same signals suppressed fat production by 22% in the C3H.B6–6T congenic mouse strain that exhibits accelerated age-related changes in body composition. In an effort to understand the means by which fat production was inhibited, irradiated mice receiving bone marrow transplants from heterozygous GFP$^+$ mice revealed that 6 weeks of these low-magnitude mechanical signals reduced the commitment of mesenchymal stem cell differentiation into adipocytes by 19%, indicating that formation of adipose tissue in these models was deterred by a marked reduction in stem cell adipogenesis. Translated to the human, this may represent the basis for the nonpharmacologic prevention of obesity and its sequelae, achieved through developmental, rather than metabolic, pathways.

mesenchymal stem cells | obesity | therapeutics | diabetes | vibration

Sixty percent of adult Americans are overweight, and obesity and diabetes threaten close to 30% of the population (1). Annually, these diseases consume more than $150 billion in health service costs, yet effective pharmacologic interventions at any scale have proven elusive (2). Even control of obesity and diabetes has proven difficult, with a principal etiologic factor being a "sedentary lifestyle" and a common therapeutic intervention being exercise (3). Although the exact mechanism remains unknown, the pathways by which exercise suppresses adipogenesis are certain to involve both metabolic (4) and mechanical (5) factors, and a more complete understanding will help define physical and physiologic pathways that may, at some point, help control the pathogenesis of these diseases (6).

It is widely accepted that exercise suppresses obesity and the onset of type II diabetes by metabolizing calories that accumulate through the diet (7) and regulating insulin, free fatty acids (FFA), and triglyceride (TG) production through physiologic control of sugar in the bloodstream (8). Thus, the inhibition of obesity and diabetes through exercise is achieved by metabolizing caloric intake via increased work expenditure (9) and a proportional reduction in hyperglycemia (10). This implies that the more strenuous and extended the exercise, the greater the benefit in metabolizing fat (11, 12). In some contrast to this "more is better" perspective, it has recently been shown that short daily durations of high-frequency, extremely low-level mechanical signals, three orders of magnitude below those induced by exercise (13), can positively influence other physiologic systems, including bone (14) and muscle (15), once thought responsive only to intense physical challenges.

Considering that adipocytes, osteoblasts, and myocytes all derive from a common progenitor, marrow-derived mesenchymal stem cells (MSCs) (16), it was hypothesized that these low-magnitude mechanical signals (LMMS), which are anabolic to the musculoskeletal system, would, in parallel, suppress adiposity. This would be achieved not by metabolizing existing adipose tissue, but instead by suppressing the differentiation of stem cells into adipocytes. Thus, adipogenesis would be curbed via a developmental pathway, and at a physical input well below that currently considered necessary to suppress adiposity via exercise (17). Finally, as evidence that this intervention could effectively influence a model genetically predisposed to adiposity, the ability of these mechanical signals to suppress fat production was examined in a congenic mouse model that recapitulates age-related changes in body composition (18).

Results

LMMS Suppression of Adiposity in Normal B6 Mice. At baseline, body weights of the LMMS (21.2 ± 1.5 g) and control (CTR) (21.1 ± 1.7 g) mice were similar ($P = 0.9$). Throughout the course of the protocol, body mass of the two groups increased at similar rates (Fig. 1). Activity patterns during the 15 min of LMMS and sham treatment were not noticeably different from their behavior in their cages or from each other. There were no noticeable differences in eating behavior between groups, and weekly food intake between LMMS (26.4 ± 2.1 g·week^{-1}) and CTR (27.0 ± 2.1 g·week^{-1}) mice was essentially identical (Fig. 1). At 12 weeks, when the *in vivo* CT scans were performed, the body mass of LMMS animals was not significantly different from CTR (4.0% lower in LMMS; $P = 0.2$) (Table 1).

As measured at 12 weeks by *in vivo* CT, fat volume in the torso of LMMS B6 mice was 27.4% lower than that measured in CTR mice ($P = 0.008$) (Fig. 2). Differences in body mass or food intake failed to account for the suppressed adipose tissue measured in the LMMS mice. Correlations between food intake and total body mass ($r^2 = 0.15$; $P = 0.7$) or fat volume ($r^2 = 0.008$; $P = 0.6$) were weak and indicated that the lower adiposity in LMMS animals could not

Author contributions: C.T.R., C.J.R., J.E.P., and S.J. designed research; C.T.R., E.C., Y.K.L., B.B., J.E.P., and S.J. performed research; H.C., D.J.N., V.M., and C.J.R. contributed new reagents/analytic tools; C.T.R., E.C., Y.K.L., B.B., J.E.P., and S.J. analyzed data; and C.T.R. wrote the paper.

Conflict of interest statement: C.T.R. is a founder of and consultant for Juvent Medical, Inc. C.T.R., S.J., and J.E.P. have submitted a provisional patent to the U.S. Patent and Trademark Office regarding the method and application of the technology.

Freely available online through the PNAS open access option.

Abbreviations: LMMS, low-magnitude mechanical signal; CTR, control; FFA, free fatty acid; NEFA, nonesterified FFA; TG, triglyceride; MSC, mesenchymal stem cell.

†To whom correspondence should be addressed. E-mail: clinton.rubin@sunysb.edu.

This article contains supporting information online at www.pnas.org/cgi/content/full/0708467104/DC1.

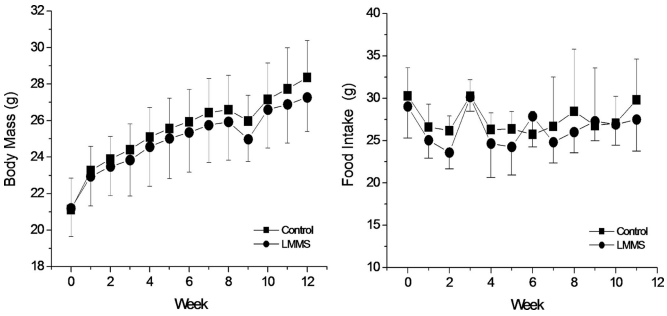

Fig. 1. Over the course of the experimental period, no significant differences were measured between average body mass of the B6 CTR (■) relative to LMMS B6 mice (●). Weekly food intake over this period was also similar between groups ($n \geq 15$ in each group).

be explained by differences in food consumption between groups. Whereas variations in body mass of the CTR mice correlated strongly with fat volume ($r^2 = 0.70$; $P = 0.0001$), no such correlation was observed in LMMS ($r^2 = 0.18$; $P = 0.1$), indicating that fat mass contributed to weight gain in CTR but did not account for the increase in body mass in the mechanically stimulated animals [supporting information (SI) Fig. 5]. Body mass as a covariate increased the P value to 0.013 whereas food intake as a covariate did not alter the P value for the difference between CTR and LMMS mice.

In contrast to fat volume, total lean volume of the torso (total volume minus fat and bone) was similar between LMMS and CTR ($P = 0.7$) (Table 1), whereas lean volume as a ratio of body mass was 5.0% greater in LMMS ($P = 0.01$). Bone volume of the skeleton, from the base of the skull to the distal region of the tibia, as a ratio of body mass was 4.6% greater in LMMS than CTR ($P = 0.03$). Fat volume normalized to body mass was 23.5% less in the LMMS ($P = 0.004$), and the ratio of fat volume to lean mass was 27.6% lower in LMMS than in CTR ($P = 0.005$). No differences in length of the tibia ($P = 0.6$) or torso ($P = 0.6$) or weight of the heart ($P = 0.7$) or liver ($P = 0.6$) were identified between groups.

Fat volume data derived from *in vivo* CT at 12 weeks were supported by the weights of the dissected fat pads harvested at 15 weeks, where LMMS had 26.2% less epididymal ($P = 0.01$) and 20.8% less subcutaneous ($P = 0.02$) fat than CTR (Table 2). Normalized to mass, there was 22.5% less epididymal and 19.5% less subcutaneous fat in LMMS than CTR ($P = 0.007$).

To account for the 1.2-g body mass difference between LMMS and CTR mice measured at 12 weeks, *in vivo* CT measurements of fat volume were converted to mass equivalents. Using a density of 0.9196 g·cm^{-3} to convert fat volume to mass (19) indicated that 3.54 ± 0.9 g of the average LMMS mouse mass came from fat (13% of total mass) whereas 4.87 ± 1.5 g of the mass of the average CTR mouse came from fat (17% of total mass). Thus, the lack of fat in the LMMS animals was, in essence, able to account for the "missing mass" between the groups ($P = 0.01$).

In parallel with the suppression of adiposity, TG in adipose tissue of LMMS mice were 21.1% ($P = 0.3$) lower than CTR and 39.1% lower in the liver ($P = 0.02$) (Fig. 3). Total nonesterified FFA (NEFA) in adipose tissue were 37.2% less in LMMS ($P = 0.01$), whereas NEFA in the liver of LMMS mice was 42.6% lower ($P = 0.02$) than CTR. Although there was a slight decrease in fasting glucose and insulin levels in the LMMS group ($P = 0.07$), this was not significantly different, suggesting that these mechanical signals had no significant effect on liver or β cell function (Table 2). Similarly, there was no significant change in glucose tolerance, insulin signaling, or fatty acid oxidation in muscle, liver, or adipose tissue (data not shown). Circulating levels of leptin were 38.3% lower in the LMMS as compared with CTR ($P = 0.07$), whereas adiponectin (down 16.3%; $P = 0.16$) and resistin (down 13%; $P = 0.17$) were not as markedly suppressed (Table 2).

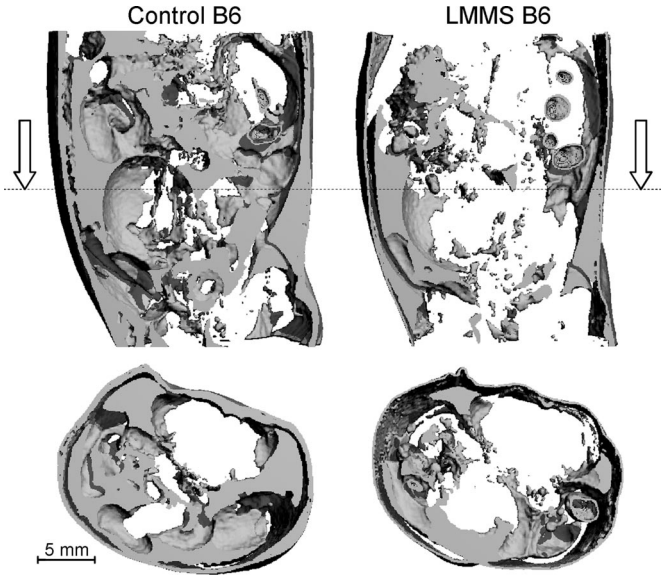

Fig. 2. A longitudinal (*Upper*) and transverse (*Lower*, at level of dotted line) reconstruction of subcutaneous and epididymal fat content through the torso of a CTR (*Left*) and LMMS (*Right*) B6 mouse, performed *in vivo* at 12 weeks by using CT signal parameters specifically sensitive to fat. After 12 weeks of LMMS, the average amount of fat within the torso was 27% lower than that of age-matched CTR.

LMMS Inhibits the Differentiation of GFP Marrow Cells into Adipocytes. It has recently been reported that the adipogenic precursors in mice are derived from bone marrow stem cells (16), an anatomic site subject to these mechanical signals (20). Thus, GFP-labeled recipient mice were used to determine whether LMMS suppressed adiposity by redirecting bone marrow-derived adipogenic stem cells. This was accomplished by examining the production of adipocytes after GFP-labeled bone marrow transplant. When the GFP$^+$ recipients were euthanized after 6 weeks of loading (animal age 15 weeks), the mass of LMMS was not significantly different from CTR (3.6% lower; $P = 0.19$). Flow cytometry demonstrated the ratio of GFP$^+$ adipocytes in the epididymal fat pad to GFP$^+$

Table 1. Body habitus parameters of CTR and LMMS B6 mice at 12 weeks

Mice	Body mass at 12 weeks, g	Fat volume, mm^3	Lean volume, mm^3	Fat volume/body mass, mm^3/g	Bone volume/body mass, mm^3/g	Lean volume/body mass, mm^3/g	Fat volume/lean mass, mm^3/g
CTR B6	28.6 ± 2.49	5,298 ± 1,671	17,265 ± 1,184	183 ± 40	18.2 ± 1.2	606 ± 36	232 ± 66
LMMS B6	27.4 ± 2.21	3,849 ± 927	17,464 ± 1,548	140 ± 31	19.0 ± 0.8	637 ± 27	169 ± 43
% difference	−4.0	−27.4	+1.2	−23.5	+4.6	+5.0	−27.6
P value	0.20	**0.008**	0.69	**0.004**	**0.030**	**0.013**	**0.005**

Data are mean and SD, as well as percentage difference and *P* values, of body habitus parameters of the CTR and LMMS B6 mice at 12 weeks as defined by *in vivo* microcomputed tomography ($n = 15$ in each group; *P* values <0.05 are in bold).

Table 2. Body habitus and biochemical parameters of CTR and LMMS B6 mice

Mice	Epididymal fat weight, g	Subcutaneous fat weight, g	Plasma insulin, ng/ml	Plasma leptin, ng/ml	Plasma adiponectin, μg/ml	Plasma resistin, ng/ml
CTR B6	0.63 ± 0.21	0.21 ± 0.06	0.54 ± 0.09	2.34 ± 1.53	6.92 ± 1.88	3.14 ± 0.95
LMMS B6	0.47 ± 0.12	0.17 ± 0.03	0.48 ± 0.07	1.44 ± 0.93	5.80 ± 2.29	2.73 ± 0.55
% difference	−26.2	−20.8	−10.8	−38.3	−16.3	−13.0
P value	**0.014**	**0.016**	0.07	0.07	0.16	0.17

Data are mean and SD, as well as percentage difference and *P* values, of body habitus ($n \geq 15$ in each group) and biochemical parameters ($n \geq 14$ in each group) of the CTR and LMMS B6 mice measured after euthanasia (*P* values <0.05 are in bold).

marrow-based MSCs to be 19% lower ($P = 0.018$) in LMMS relative to CTR (SI Fig. 6). These data indicating reduced commitment to adipocytes were supported by the weight of the epididymal fat pad after 6 weeks of LMMS, which was 12.2% less than CTR ($P = 0.029$).

LMMS Suppresses Age-Related Changes in Fat Composition. 6T mice were subjected to LMMS to determine whether these mechanical signals could suppress this animal's predisposition to age-related deterioration of body composition (18). At 9 weeks (16 weeks of age), 6T mice subject to LMMS were 3.9% lighter ($P = 0.19$) (Table 3), and had 21.6% less fat volume ($P = 0.02$) (Fig. 4) than CTR. NEFA in adipose tissue were 48.0% less in LMMS ($P = 0.02$), whereas TG were 25.0% lower ($P = 0.27$). Whereas NEFA in the liver was not influenced by LMMS (4.8% lower; $P = 0.69$), TG realized a 15.3% reduction by the mechanical signal ($P = 0.002$).

Discussion

Obese children are more prone to develop type II diabetes (21) and increase their lifetime risk of cardiovascular disease (22). Overweight adults, not yet even obese, are more susceptible to chronic, debilitating diseases and increased risk of death (23). Although exercise remains the most readily available and generally accepted means of curbing weight gain and the onset of type II diabetes, compliance is poor, and the means by which these metabolic and mechanical cues conspire to suppress adiposity and diabetes are not fully understood. In contrast to the perception that physical signals must be large and endured over long periods of time to offset caloric input and control insulin production, the results presented here indicate that the cell population(s) and physiologic process(es) responsible for establishing fat mass and, perhaps indirectly, FFA and TG production are readily influenced by brief exposure to mechanical signals barely large enough to be perceived.

From a metabolic perspective, the trend toward improved glucose tolerance measured here indicates that the metabolic machinery of the organism has been elevated, and perhaps remains higher even after LMMS has subsided, suggesting that a mechanosensory element within the cell population has been triggered without the signals being large (24). And rather than requiring an accumulation of mechanical information over an aggregate of time to elevate metabolic activity, perhaps these cell populations are endowed with a memory, or refractory period, in which their metabolic machinery, once triggered, remains active even after the stimulus has subsided (25).

Somewhat contrary to a "metabolic" perspective, the low intensity of the daily regimen indicates that the inhibition of adipogenesis is achieved by pathways other than an exercise-mediated increase in metabolic activity. Indeed, the GFP^+ recipient mice indicate that the reduced adiposity resulting from LMMS is achieved in part by influencing the differentiation of fat precursors, deterring MSCs from committing to an adipocytic lineage. Even the 6T mouse predisposed to age-related changes in body composition responded to LMMS by suppressed adiposity. Considered in the context of previous evidence that LMMS is anabolic to bone (26) and muscle

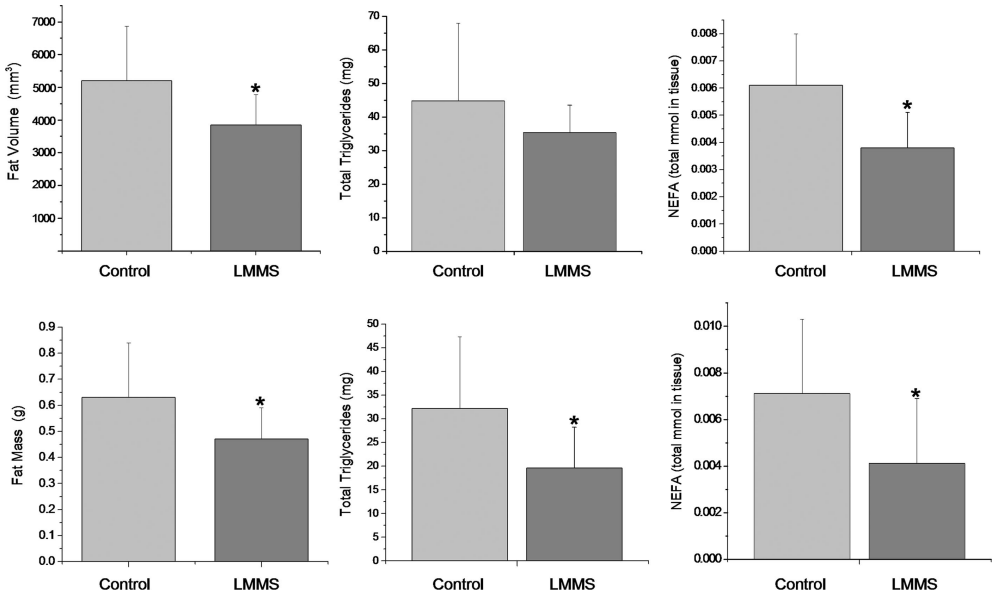

Fig. 3. A summary of phenotypic and biochemical differences between LMMS and CTR B6 mice indicates that LMMS reduces risk factors associated with diabetes. Mean and SD of fat volume in the torso of CTR and LMMS B6 mice, as measured by CT scan (*Upper Left*), as well as by mass of the epididymal fat pad (*Lower Left*). Also shown are total TG (*Upper Center*) and NEFA in adipose tissue (*Upper Right*) and TG and NEFA in liver (*Lower*). $n = 15$ in each group for the CT scans and epididymal mass, $n = 8$ for measurements in adipose tissue, and $n = 12$ for the liver. *, $P < 0.05$.

Table 3. CTR and LMMS 6T body habitus and biochemical parameters in plasma and tissues

Mice	Body mass at 9 weeks, g	Fat volume, mm^3	Adipose tissue NEFA, μmol/mg protein	Adipose tissue TG, μg/mg protein	Liver NEFA, μmol/mg protein	Liver TG, μg/mg protein
CTR 6T	20.43 ± 1.27	343.6 ± 59.2	0.19 ± 0.04	2,005.5 ± 656.4	0.0076 ± 0.0014	51.51 ± 0.77
LMMS 6T	19.63 ± 0.93	269.2 ± 52.5	0.10 ± 0.04	1,503.8 ± 474.8	0.0073 ± 0.0011	43.6 ± 2.67
% difference	−3.9	−21.6	−48.0	−25.02	−4.82	−15.3
P value	0.19	**0.02**	**0.02**	0.27	0.67	**0.002**

Data are mean and SD, as well as percentage difference and *P* values, for the CTR and LMMS 6T body habitus parameters as measured by CT at week 9 of the protocol ($n = 8$ in each group) and biochemical parameters in plasma ($n = 8$ in each group) and tissues ($n = 4$ in each group), measured directly after euthanasia (*P* values <0.05 are in bold). Note that the fat volume is for a specific region of the abdomen, and not the fat volume for the entire animal.

tissues (15), our data suggest that LMMS may drive MSCs to enhance the musculoskeletal system by encouraging noncommitted stem cell precursors toward a connective tissue lineage. The common heritage of these cell systems suggest that conditions of fat gain or bone loss could be controlled by targeting the precursors of adipocytes and osteoblasts.

Previous studies have shown that plasma levels of leptin correlate with the degree of adiposity, whereas the adipokines adiponectin and resistin more closely correlate with changes in metabolic state (27). The reduction in circulating leptin levels in the B6 LMMS mice as compared with CTR is consistent with a decrease in adipose tissue mass, whereas the absence of a significant change in either adiponectin or resistin levels supports a conclusion that the reduced adiposity was achieved without altering the metabolic state of the animals.

Among the limitations of these experiments is the range of time periods examined, making it difficult to directly compare them against each other (SI Fig. 7). Although each protocol was designed to address a different question, LMMS suppressed adiposity across all protocols, as measured by both fat mass and fat volume. Longer protocols (e.g., 1 year) will be necessary to determine whether the suppression of fat mass, TG, and NEFA levels persist, and shorter-term protocols (e.g., 1 week) must be developed to identify the molecular regulators of the response. Finally, more expansive protocols must be used to assess whether altered adipogenesis is correlated to changes in the quantity and quality of the musculoskeletal system.

There is recent *in vitro* evidence that high levels of mechanical stretch can direct MSCs toward an osteoblastogenic lineage, in preference over adipocytes (28). Here, in an *in vivo* system, we were able to demonstrate that physical signals need not be large to influence differentiation pathways and can be delivered noninvasively to influence the phenotype of the entire animal. Rather than requiring high levels of mechanical distortion or damage to determine their fate, perhaps these stem cell populations are sensitive to frequency-specific stimuli, similar to other physiologic systems designed to monitor "exogenous signals," such as vision (color), hearing (tone), and tactile sense (pressure), and that these physical signals are processed within specific windows of sensitivity and may begin to shut down when the signal becomes too bright, too loud, or too heavy. Certainly, when considered in the context of the exceedingly small tissue strains that arise from the mechanical signals used here, perhaps the critical component of mechanotransduction should be considered the acceleration, rather than distortion, as an efficient means of notifying a cell population of physical challenges (29).

In any case, the inhibition of adipogenesis by LMMS, considered in parallel with their anabolic potential in bone and muscle (15), supports the presence of a systems-interdependent benefit of exercise and the systemic consequences of a sedentary lifestyle. In hindsight, perhaps this should not be so surprising, because bone and muscle are well known to positively respond to mechanical challenges, whereas fat thrives with inactivity. Arguably, these data indicate that mesenchymal precursors perceive and respond to mechanical "demands" as stimuli to differentiate down a musculoskeletal pathway rather than "defaulting" to adipose tissues and may, to a certain extent, etiologically interconnect age-related increases in obesity, osteopenia, and sarcopenia.

The physiologic relevance of LMMS becomes evident upon examination of the contractile spectra of muscle. Type IIa muscle fibers fire in the range of 20–50 Hz (30), and, albeit small in amplitude relative to the peak signals generated by strenuous activities such as running, these higher-frequency signals are, over time, a predominant component of the mechanical energy in the musculoskeletal system (31). Conditions such as aging reduce these higher-frequency domain signals (32) and suggest that the age-

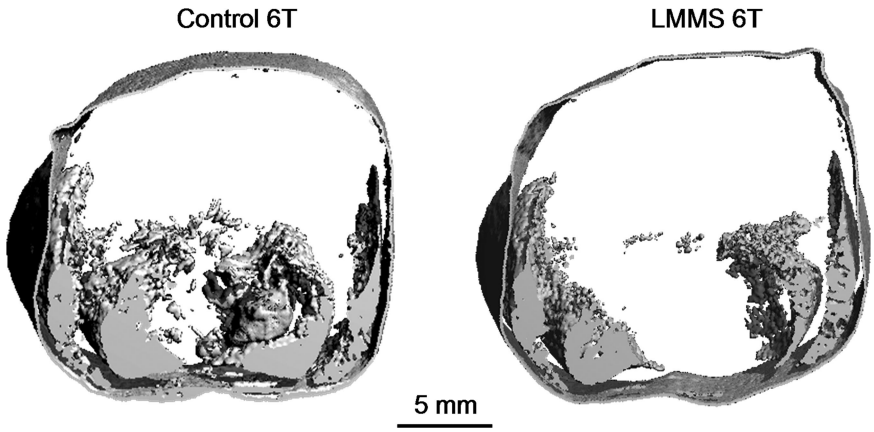

Fig. 4. Transverse CT reconstruction performed *in vivo* at 9 weeks, with signal sensitivity to adipose tissue, showing fat content through the abdominal region of the torso of a CTR (*Left*) and LMMS (*Right*) female 6T mouse. No significant difference in body mass was evident between LMMS and CTR 6T (3.9% less in LMMS), but adipose within the torso was 22% lower in mechanically stimulated animals ($P = 0.02$).

related bone wasting and increase in adiposity may occur not only from diminished peak-load-bearing capacity, but the dissolution of low-level signals caused by the sarcopenia that parallels these conditions (33).

In parallel with the lower adiposity realized by LMMS, TG and NEFA in adipose and liver tissue, key biochemical factors related to type II diabetes, were suppressed in both the B6 and 6T mouse. Numerous studies have demonstrated that dyslipidemia can have major negative impact on metabolism, growth, and development. In particular, intratissue lipid accumulation (liver steatosis) and intramyocellular lipids have been closely linked to insulin resistance and are considered the best predictor for the future development of insulin resistance (34). Although obesity results in states of dyslipidemia, lipodystrophy (the absence of adipose tissue deposits) can have the same negative consequence because of limited peripheral FFA and TG storage capacity (35). Thus, a physiologic balance between lipid storage and lipid release must be maintained for optimum metabolism. The ability to suppress adipose tissue expansion by mechanical signals, as well as limit NEFA and TG production, may provide a simple, nonpharmacologic approach to limit obesity in a manner sufficient to prevent the consequences of dyslipidemia.

LMMS were delivered to the mouse via whole-body vibration. When considering translating this to the clinic, it is important to note that associations persist between vibration and adverse health conditions, including low-back pain, cartilage erosion, circulatory disorders, and neurovestibular dysfunction (36), leading to International Safety Organization advisories to limit human exposure to these mechanical signals (37). At the frequency (90 Hz) and amplitude (0.2-*g* peak) used in these studies, the exposure would be considered safe for >4 h each day.

In summary, our findings indicate that brief exposure to high-frequency LMMS markedly suppress adipogenesis and TG and NEFA production and could lead to a unique, nonpharmacologic intervention for the control of obesity and its sequelae, such as type II diabetes. The fact that the signals are so low, and so brief, yet with such striking response in the phenotype of both the growing animal and a model of accelerated aging, suggests a means of suppressing adipogenesis independent of a metabolic pathway. That a mechanical signal anabolic to bone may simultaneously inhibit fat production would couple the prevention of obesity to the prevention of osteoporosis, achieved by controlling differentiation of MSCs rather than the resident cells in adipose or skeletal tissue.

Methods

All procedures were reviewed and approved by the Stony Brook University animal care and use committee. The overall experimental design consisted of three distinct protocols, each designed around a different time scale to examine specific components of the general hypothesis (SI Fig. 7). The first protocol, to determine whether LMMS can suppress adiposity in normal male mice as compared with CTR, began with young adult mice 7 weeks of age and required a 15-week protocol to ensure that differences in fat production between groups could be assayed. The second protocol, to examine the influence of LMMS on the differentiation of MSCs, was shorter (6 weeks of loading), allowing an earlier evaluation of stem cell commitment to adipocytes. Precise irradiation dosing, dependent on animal mass, required that each mouse be at least 8 weeks of age, and considerations for animal health required that this be followed by a week of recovery before handling. Thus, the animals began the LMMS protocol at 9 weeks of age and were euthanized at 15 weeks of age. The third protocol, to examine whether LMMS could suppress adipogenesis in a congenic mouse model prone to adiposity, began when the animals were 7 weeks old (as in the first experiment). To facilitate comparison of body habitus data to those reported in the literature (18), this group was euthanized at 16 weeks of age after 9 weeks of LMMS.

Mechanical Influence on Adiposity in the Normal Mouse. Forty C57BL/6J (B6) male mice, 7 weeks of age and given free access to a normal chow diet, were randomly separated into two groups: those subjected to brief periods of LMMS ($n = 20$) or their age-matched sham CTR ($n = 20$). Animal weights, as well as their individual food consumption, were measured weekly. For 15 weeks, 5 days per week, LMMS mice were subjected to 15 min of a 90-Hz, 0.2-*g* peak acceleration (1.0 g = Earth's gravitational field, or 9.8 $m \cdot s^{-2}$), induced by vertical whole-body vibration via a closed-loop feedback controlled, oscillating platform (modified from Juvent Medical, Inc., Somerset, NJ) (38). A sinusoidal vibration at this magnitude and frequency causes a displacement of ≈ 12 μm and is barely perceptible to human touch. CTR animals were placed on an inactive platform each day.

At 12 weeks into the protocol (19 weeks of age), *in vivo* microcomputed tomography (VivaCT 40; Scanco, Bassersdorf, Switzerland) was used to quantify fat and lean volume of the torso ($n = 15$ in each group) (39). The torso of each mouse was CT scanned at an isotropic voxel size of 76 μm (45 kV, 133 μA, 300-ms integration time). Torso length was defined by two anatomical landmarks, from the distal tibia to the base of the skull. Image segmentation was calibrated by using the density range of a fresh fat pad from a B6 mouse unrelated to this study. Gaussian filtering was applied ($\sigma = 1.5$; support = 3.0) to reduce image noise before scans were evaluated for volume.

At 15 weeks into the protocol (22 weeks of age) mice were fasted overnight, and blood collection was performed by cardiac puncture with the animal under anesthesia and plasma harvested by centrifugation (14,000 rpm, 15 min, 4°C). Mice were euthanized by cervical dislocation, and the different tissues (i.e., epididymal fat pad and subcutaneous fat pads from the torso, liver, and heart) were excised, weighed, frozen in liquid nitrogen, and stored at −80°C.

Glycerol, TG, FFA, insulin, and three adipokines (leptin, adiponectin, and resistin) were measured in the plasma ($n \geq 14$ per group). TG and NEFA were measured on lipid extracts from adipose tissue ($n = 8$ per group) and liver ($n = 12$ per group). Plasma insulin levels and adipokines were measured by using ELISA kits (Mercodia, Winston-Salem, NC; and Linco Research and Millipore, Chicago, IL, respectively). TG and FFA/NEFA from plasma and tissues were measured by using enzymatic colorimetric kits (Serum Triglyceride Determination Kit from Sigma, Saint Louis, MO; and NEFA C from Wako Chemicals, Richmond, VA). Total lipids from white adipose tissue (epididymal fat pad) and liver were extracted and purified following the chloroform–methanol method with some modifications (40).

GFP-Labeled Stem Cells. To determine whether LMMS influenced the differentiation pathway of adipocyte precursors, we used a model of bone marrow transplantation using heterozygous C57BL/6J (B6) GFP^+ mice as bone marrow donors. The GFP expression in these transgenic mice is under the control of a constitutive actin promoter; therefore, all cells within the animal should produce GFP protein. Once implanted into a normal mouse that does not endogenously express GFP, the fate of the bone marrow stem cells can be monitored by the production of GFP. Targeted as recipients, 16 wild-type male C57BL/6J (B6) mice, 8 weeks of age, were irradiated in a γ cell irradiator with a Cs137 source at a total dose of 15 Gy (dose rate of 1.07 Gy/min). This whole-body exposure had been previously determined to be lethal to animals of this age unless they received, within 24 h, a bone marrow transplant from a healthy donor. The following day, irradiated mice were injected through the tail vein with 1×10^7 cells (total injection of 100 μl) harvested from the bone marrow of the GFP^+ donor mice (41).

After 1 week of recovery, half of the GFP^+ recipient mice ($n = 8$) were subjected to LMMS (as above), and half served as age-matched sham-loaded CTR ($n = 8$). Animals were euthanized at 6 weeks of the protocol, and the epididymal fat pad and marrow

PHYSIOLOGY

from the tibia were harvested for examination. Adipocytes and bone marrow cells isolated from the GFP^+ transplanted mice were analyzed by using the GFP fluorescence signal.

FACS analysis was performed on single-cell suspensions from the direct isolation of the marrow and fat tissues. Adipocytes were isolated from the epididymal fat pad by mechanical and collagenase digestion in KRH buffer, centrifuged to remove the stromal vascular compartment, and then resuspended in PBS. The cell population in the marrow was collected by clipping both ends of the tibia and flushing out the marrow with PBS (0.5% BSA). Red cells were removed by incubation with lysis buffer, and the pellet of white cells was resuspended in PBS. Samples were fixed in PBS at a final concentration of 1.5% formalin, protected from light, and stored at 4°C for up to 1 week before analysis.

Flow cytometry data were collected by using a FACScan flow cytometer (Becton Dickinson, San Jose, CA). For adipocyte samples, percentages were calculated based on 2,500 gated events, and the percentage of positively stained cells was determined. For each bone marrow sample, 10,000 gated events were collected. To help identify MSCs within the overall cell population of the marrow, all cells were exposed to stem cell antigen-1 (Sca-1), an antigen previously associated with hematopoietic cells but subsequently demonstrated to exhibit adipogenic, chondrogenic, and osteogenic potential (42). Phycoerythrin-conjugated rat anti-mouse Sca-1 antibody and isotype CTR (BD Biosciences, San Jose, CA) were used at 1:100 dilution in PBS with 0.01% sodium azide.

Mouse Model That Recapitulates Age-Related Changes in Body Composition. To determine whether LMMS can influence an animal model with a genetically driven predisposition to adiposity, 18 female C3H.B6–6T (6T) mice, 7 weeks of age, were obtained from The Jackson Laboratory (Bar Harbor, ME). The 6T is a congenic mouse strain derived by transferring a small genomic region of mouse chromosome 6 from C3H/HeJ onto a C57BL/6J (B6) background for 10 generations. The mice were initially generated to map a major quantitative trait locus for circulating IGF1 and to understand the physiologic and body composition changes associated with accelerated aging (18). The phenotypic characteristics of the 16-week female 6T mouse include reduced circulating and hepatic IGF1 and increased adiposity despite similar body weights compared with the parental B6 mouse (43). 6T mice were subjected to a 9-week loading and analysis similar to that described for the B6 long-term experiments, except that CT, performed just before euthanasia, was spatially limited to measure only the volume of the abdominal region.

We thank B. Lee, C. Bastie, S. Lublinsky, and E. Ozcivici for help with animal imaging and tissue processing. This work was supported by National Institutes of Health Grants AR 43498, AR 45433, and DK33823; National Aeronautics and Space Administration Grant NAG 9-1499; The Goldman Foundation; and a W. H. Coulter Translational Research Award.

1. Carmona R (July 16, 2003) *The Obesity Crisis in America, U.S. Surgeon General Testimony Before the Subcommittee on Education Reform Committee on Education and the Workforce* (Dept of Health and Human Services, Washington, DC).
2. Lazar MA (2005) *Science* 307:373–375.
3. Nassis GP, Papantakou K, Skenderi K, Triandafillopoulou M, Kavouras SA, Yannakoulia M, Chrousos GP, Sidossis LS (2005) *Metabolism* 54:1472–1479.
4. Atlantis E, Barnes EH, Singh MAF (2006) *Int J Obes* 30:1027–1040.
5. Tanabe Y, Koga M, Saito M, Matsunaga Y, Nakayama K (2004) *J Cell Sci* 117:3605–3614.
6. Baynard T, Franklin RM, Goulopoulou S, Carhart R, Jr, Kanaley JA (2005) *Metabolism* 54:989–994.
7. Dehghan M, Akhtar-Danesh N, Merchant AT (2005) *Nutr J* 4:24.
8. Stumvoll M, Goldstein BJ, van Haeften TW (2005) *Lancet* 365:1333–1346.
9. Frank LL, Sorensen BE, Yasui Y, Tworoger SS, Schwartz RS, Ulrich CM, Irwin ML, Rudolph RE, Rajan KB, Stanczyk F, *et al.* (2005) *Obes Res* 13:615–625.
10. Colombo M, Gregersen S, Kruhoeffer M, Agger A, Xiao J, Jeppesen PB, Orntoft T, Ploug T, Galbo H, Hermansen K (2005) *Metabolism* 54:1571–1581.
11. Slentz CA, Aiken LB, Houmard JA, Bales CW, Johnson JL, Tanner CJ, Duscha BD, Kraus WE (2005) *J Appl Physiol* 99:1613–1618.
12. Centers for Disease Control and Prevention (2005) *Morbid Mortal Wkly Rep* 54:1208–1212.
13. Xie L, Jacobson JM, Choi ES, Busa B, Donahue LR, Miller LM, Rubin CT, Judex S (2006) *Bone* 39:1059–1066.
14. Rubin C, Turner AS, Bain S, Mallinckrodt C, McLeod K (2001) *Nature* 412:603–604.
15. Gilsanz V, Wren TA, Sanchez M, Dorey F, Judex S, Rubin C (2006) *J Bone Miner Res* 21:1464–1474.
16. Crossno JT, Jr, Majka SM, Grazia T, Gill RG, Klemm DJ (2006) *J Clin Invest* 116:3220–3228.
17. Lakka TA, Bouchard C (2005) *Handb Exp Pharmacol*, 137–163.
18. Rosen CJ, Ackert-Bicknell CL, Adamo ML, Shultz KL, Rubin J, Donahue LR, Horton LG, Delahunty KM, Beamer WG, Sipos J, *et al.* (2004) *Bone* 35:1046–1058.
19. Watts GF, Chan DC, Barrett PH (2002) *Metabolism* 51:1206–1210.
20. Qin YX, Kaplan T, Saldanha A, Rubin C (2003) *J Biomech* 36:1427–1437.
21. Cara JF, Chaiken RL (2006) *Curr Diabetes Rep* 6:241–250.
22. Freedman DS, Mei Z, Srinivasan SR, Berenson GS, Dietz WH (2007) *J Pediatr* 150:12–17.
23. Adams KF, Schatzkin A, Harris TB, Kipnis V, Mouw T, Ballard-Barbash R, Hollenbeck A, Leitzmann MF (2006) *N Engl J Med* 355:763–778.
24. Rubin J, Rubin C, Jacobs CR (2006) *Gene* 367:1–16.
25. Skerry TM, Bitensky L, Chayen J, Lanyon LE (1988) *J Orthop Res* 6:547–551.
26. Judex S, Zhong N, Squire ME, Ye K, Donahue LR, Hadjiargyrou M, Rubin CT (2005) *J Cell Biochem* 94:982–994.
27. Silha JV, Weiler HA, Murphy LJ (2006) *Obesity (Silver Spring)* 14:1320–1329.
28. David V, Martin A, Lafage-Proust MH, Malaval L, Peyroche S, Jones DB, Vico L, Guignandon A (2007) *Endocrinology* 148:2553–2562.
29. Garman R, Gaudette G, Donahue LR, Rubin C, Judex S (2007) *J Orthop Res* 25:732–740.
30. Person RS, Kudina LP (1972) *Electroencephalogr Clin Neurophysiol* 32:471–483.
31. Fritton SP, McLeod KJ, Rubin CT (2000) *J Biomech* 33:317–325.
32. Huang RP, Rubin CT, McLeod KJ (1999) *J Gerontol A Biol Sci Med Sci* 54:B352–B357.
33. Rosenberg IH (1997) *J Nutr* 127:990S–991S.
34. Unger RH (2003) *Endocrinology* 144:5159–5165.
35. Petersen KF, Shulman GI (2006) *Am J Med* 119:S10–S16.
36. Magnusson ML, Pope MH, Wilder DG, Areskoug B (1996) *Spine* 21:710–717.
37. International Standards Organization (1985) *Evaluation of Human Exposure to Whole-Body Vibration, ISO 2631/1* (International Standards Organization, Geneva, Switzerland).
38. Fritton JC, Rubin CT, Qin YX, McLeod KJ (1997) *Ann Biomed Eng* 25:831–839.
39. Bastie CC, Zong H, Xu J, Busa B, Judex S, Kurland IJ, Pessin JE (2007) *Cell Metab* 5:371–381.
40. Folch J, Lees M, Sloane GH (1957) *J Biol Chem* 226:497–509.
41. Biankin SA, Collector MI, Biankin AV, Brown LJ, Kleeberger W, Devereux WL, Zahnow CA, Baylin SB, Watkins DN, Sharkis SJ, *et al.* (2007) *Pathology* 39:247–251.
42. Hachisuka H, Mochizuki Y, Yasunaga Y, Natsu K, Sharman P, Shinomiya R, Ochi M (2007) *J Orthop Sci* 12:161–169.
43. Rosen CJ, Ackert-Bicknell C, Beamer WG, Nelson T, Adamo M, Cohen P, Bouxsein ML, Horowitz MC (2005) *Pediatr Nephrol* 20:255–260.